

Reconfiguration Algorithms for Cubic Modular Robots with Realistic Movement Constraints

MIT–NASA Space Robots Team¹

Massachusetts Institute of Technology, Cambridge, MA, USA

NASA Ames Research Center, Moffett Field, CA, USA

Josh Brunner ✉

Massachusetts Institute of Technology, Cambridge, MA, USA

Kenneth C. Cheung ✉

NASA Ames Research Center, Moffett Field, CA, USA

Erik D. Demaine ✉ 

Massachusetts Institute of Technology, Cambridge, MA, USA

Jenny Diomidova ✉


Massachusetts Institute of Technology, Cambridge, MA, USA

Christine Gregg ✉

NASA Ames Research Center, Moffett Field, CA, USA

Della H. Hendrickson ✉

Massachusetts Institute of Technology, Cambridge, MA, USA

Irina Kostitsyna ✉ 

KBR at NASA Ames Research Center, Moffett Field, CA, USA

Abstract

We introduce and analyze a model for self-reconfigurable robots made up of unit-cube modules. Compared to past models, our model aims to newly capture two important practical aspects of real-world robots. First, modules often do not occupy an exact unit cube, but rather have features like bumps extending outside the allotted space so that modules can interlock. Thus, for example, our model forbids modules from squeezing in between two other modules that are one unit distance apart. Second, our model captures the practical scenario of many passive modules assembled by a single robot, instead of requiring all modules to be able to move on their own.

We prove two universality results. First, with a supply of auxiliary modules, we show that any connected polycube structure can be constructed by a carefully aligned plane sweep. Second, without additional modules, we show how to construct any structure for which a natural notion of external feature size is at least a constant; this property largely consolidates forbidden-pattern properties used in previous works on reconfigurable modular robots.

2012 ACM Subject Classification Theory of computation → Computational geometry

Keywords and phrases Modular robotics, programmable matter, digital materials, motion planning

Digital Object Identifier 10.4230/LIPIcs.SWAT.2024.34

Related Version *Full Version*: <https://arxiv.org/abs/2405.15724>

1 Introduction

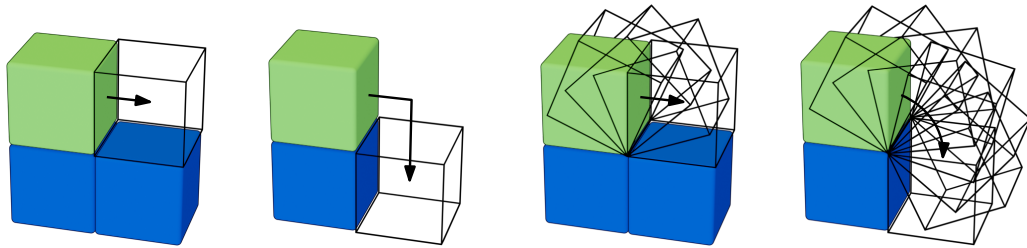
Algorithmic shape formation with self-reconfigurable modular robots has attracted significant interest by the computational geometry community in the past two decades [16, 2, 7, 9, 8, 10, 6, 34, 17, 24, 29, 4, 3, 5, 15, 12, 13, 25, 18, 28, 27]. In general, the idea is to build a

¹ Artificial first author to highlight that the other authors (in alphabetical order) worked as an equal group. Please include all authors (including this one) in your bibliography, and refer to the authors as “MIT–NASA Space Robots Team” (without “et al.”).



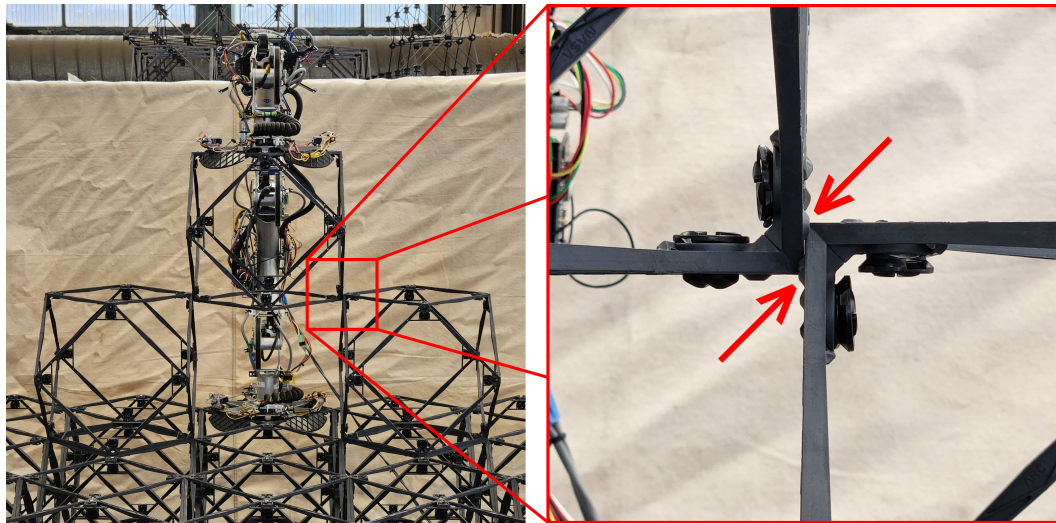
self-reconfigurable “robot” out of n identical modules, each of which can move in some way relative to its neighbors, subject to some constraints like maintaining global connectivity. This approach enables the robot to drastically change its overall shape, often with algorithmic universality results showing that any shape is possible, up to some constant feature size and/or forbidden small patterns. Real-world modular robots have been built by multiple robotics groups [31, 11, 33, 21, 32, 36], with the ultimate goal of building “programmable matter”: objects that can arbitrarily change their shape.

Sliding cubes. One of the first and simplest models for modular robot reconfiguration is *sliding squares* in 2D [16] or *sliding cubes* in 3D [2, 1]. Each module is a unit square/cube placed at a node of a square/cube lattice, and the modules must at each step have a connected dual graph (according to facet adjacencies). Figure 1 illustrates the two possible moves: (1) *straight slide* moves a (green) module to an adjacent empty location along two faces of a pair of adjacent (blue) modules; and (2) *corner slide* moves a (green) module to an adjacent empty location, and immediately turning the 90° corner around its original (blue) neighbor, moves the module one more unit to restore the adjacency with the neighbor. This model enables universal reconfiguration between polyominoes/polycubes, with $\Theta(n^2)$ moves necessary and sufficient in the worst case for 2D [16] and (in a recent breakthrough) for 3D [1, 23].



■ **Figure 1** The two moves in the sliding-cubes model. Left: straight slide. Right: corner slide. ■ **Figure 2** The two moves in the pivoting-cubes model. Left: straight pivot. Right: corner pivot.

Pivoting cubes. Another extensively studied model for modular robot reconfiguration is the *pivoting squares/hexagons* in 2D [13, 3, 4] and *pivoting cubes* in 3D [34, 17, 24]. In the pivoting-cube model, a module can move by rotating around a common edge shared with an adjacent module. Similarly to the previous model, a module moves to an adjacent empty location or to an empty location around the corner of an adjacent module (see Figure 2). However, unlike in the sliding-cube model, for a pivoting move to be valid, all cells of the grid intersected by the pivoting module must remain empty. Existing results rely on the definition of so called *forbidden pattern*, that is, a specific constant-size configuration of empty and non-empty cells, whose existence may block a possible reconfiguration. Specifically, the forbidden patterns are of the form: for any $k_1 \times k_2 \times k_3$ (for specific small values of k_1 , k_2 , and k_3) axis aligned bounding box of grid cells with two modules present in the two diagonally opposite corners of the box, the remaining cells of the box must not be empty. The set of forbidden patterns consists of the $3 \times 1 \times 1$ -pattern (two modules with a single empty cell in between), the $2 \times 2 \times 1$ -pattern (two edge adjacent modules with no other mutually adjacent modules), and the $3 \times 2 \times 1$ -pattern. The series of works on reconfiguration in the pivoting-cube model [34, 17, 24] resulted in a universal reconfiguration algorithm for a class of shapes that do not contain any of the three forbidden patterns.



■ **Figure 3** Photograph of ARMADAS robot attempting to place a module between two modules and failing due to collisions of mechanical alignment features (red arrows).

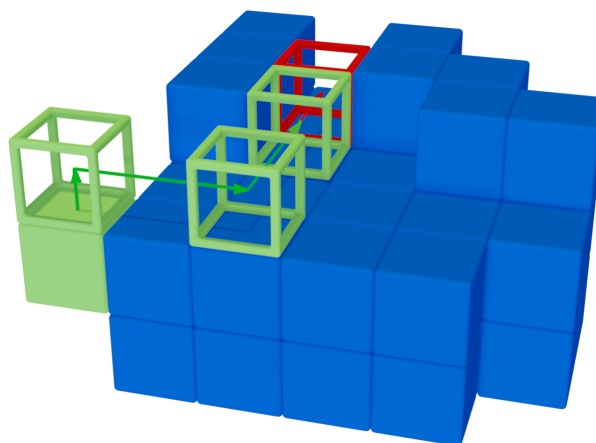
1.1 Our Model

In this paper, we introduce a new model for modular robot reconfiguration that aims to capture two important practical aspects of real-world systems, motivated by our experience with the robots and structural modules of the NASA Ames Automated Reconfigurable Mission Adaptive Digital Assembly Systems (ARMADAS) project [30]. Our model is a refinement of the sliding-cubes model, adding constraints to the moves. Notably, the constraints on the moves in our model are strictly stronger than in the pivoting-cube model as well. Thus our universality results can be seen as strengthenings of past work to better apply to real-world robotics.

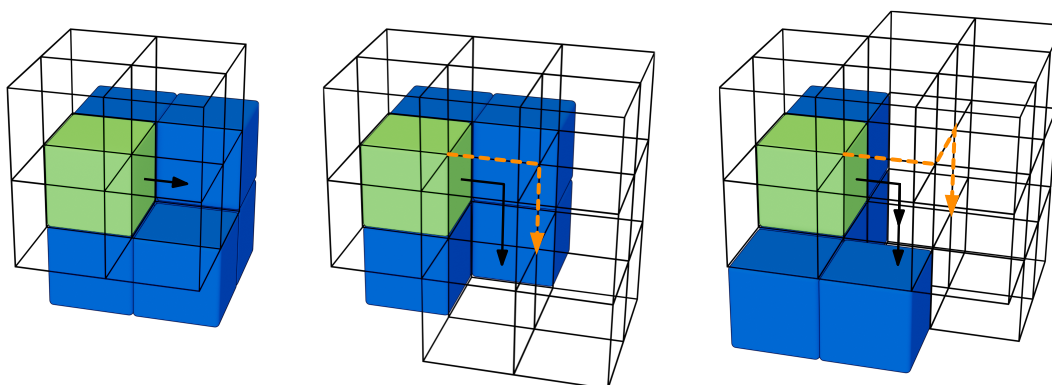
Loose sliding. The first practical issue we address is that modules typically need more room than a unit cube to actually move without collision. Figure 3 shows an example of this issue in the context of ARMADAS. To enable secure and precise relative positioning of adjacent modules, modules often have mechanical alignment features (matching bumps and indentations) that extend outside the bounding box. Having these features integrated into modules allows for high-precision, high-repeatability, and high-throughput manufacturing processes such as injection molding to make high-quality connections, rather than requiring the added complexity and weight of active attachment mechanisms [14, 20].

To avoid collision between modules with these bumps, modules need to move slightly away from neighboring modules before sliding to an adjacent cell. Thus a moving module needs the space to move a small distance away from its neighbors. In particular, it is impossible for a module to pass through a unit-wide gap between two other modules; see Figure 4.

We formalize this requirement as the *loose-sliding* constraint (refer to Figure 5): a moving module must at all times be within an otherwise empty $2 \times 2 \times 2$ cube in space that moves continuously (or equivalently, moves in unit axis-aligned steps on a grid). In other words, each unit step taken by the moving module (one for a straight slide, two for a corner slide) must have both its start and end positions within a common $2 \times 2 \times 2$ cube empty of other modules; in addition, in the case of a corner slide, the first $2 \times 2 \times 2$ empty cube must be translatable (continuously or in unit axis-aligned steps) to the second $2 \times 2 \times 2$ empty



■ **Figure 4** Valid (green) and invalid (red) moves of the green module in the loose-sliding model.

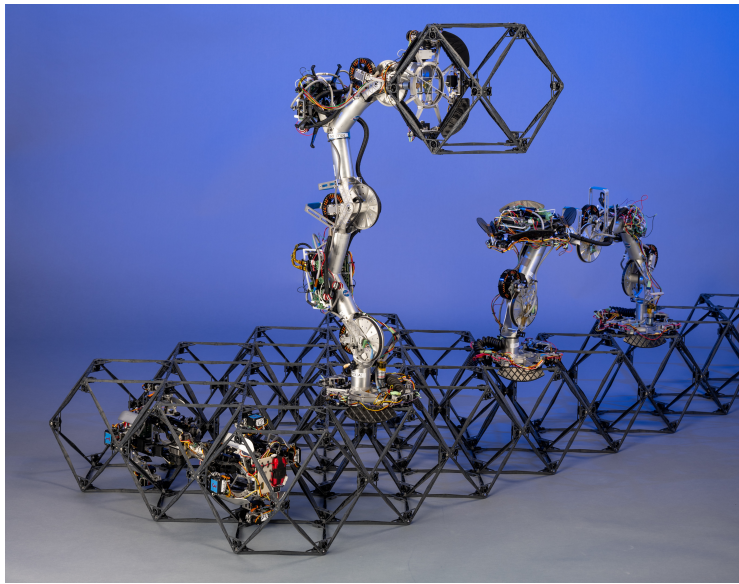


■ **Figure 5** Valid moves in the loose-sliding model. Left: straight slide move and the corresponding $2 \times 2 \times 2$ empty cube. Middle and right: corner slide move and the corresponding translation (indicated by the orange paths) of the $2 \times 2 \times 2$ empty cube.

cube while remaining empty of other modules throughout the translation. In particular, loose sliding prevents a module from sliding into a unit-wide gap between two other modules, because such a gap is not contained in an empty $2 \times 2 \times 2$ cube. More generally, we can define *k-loose sliding* to require a $k \times k \times k$ empty cube surrounding the moving module.

Passive modules via accessible sliding. The second practical issue is that modular reconfigurable robots do not scale well. Each module must have its own power, processor, networking, attachment mechanisms, and movement actuators. This module complexity limits the number of modules and practicality of the programmable matter dream.

A more recent alternative approach [30, 22, 35] is to have two types of modules: many passive/static modules that cannot move on their own and primarily serve structural purposes, and a smaller number of robots (even one) that can pick up, carry, place, and attach passive modules. Figure 6 shows this approach in action in the context of the ARMADAS project, where the primary goal is to assemble passive parts into a desired geometry – a digital cellular solid [14, 19]. (Of course, disassembly and reconfiguration is also possible.) The moving robots are more complicated than the passive modules, and thus are naturally a little larger. The simplicity of passive modules enables them to be cheaply constructed in large numbers, vastly increasing applicability [20].



■ **Figure 6** Photograph of ARMADAS robots operating in the laboratory. Each of the external robots has two primary “hands”, and can hold onto the already-built structure with either hand while moving the other hand. The right robot is carrying a module via a third hand on its back; this module can be added to the structure by another robot, such as the left robot.

Instead of explicitly modeling both moving robot(s) and passive modules, which would vastly complicate the model, we show how to obtain a similar effect via a small tweak to the loose-sliding-cubes model. Specifically, define a slide to be ***k-accessible*** if it is both *k-loose* (i.e. is the only module in some otherwise empty $k \times k \times k$ cube), and also that that $k \times k \times k$ is connected to infinity via a path of $k \times k \times k$ empty cubes, both before and after the move. Such a module can be reached by a moving robot on the outside of the shape, removed and picked up by the robot, and then placed and attached in the new location. Thus any sequence of *k-accessible* moves can be simulated by passive modules plus one moving robot whose size is at most $k \times k \times k$.

Our algorithms for sliding cubes satisfy this *k-accessible* property. Thus they are equally suitable for both modular robot reconfiguration (where every module can move on its own) and a hybrid system of passive modules and one or more moving robots. By contrast, all past sliding-cube algorithms [16, 2, 1] do not satisfy the accessible property. Indeed, *no* universal algorithm without extra modules can be accessible (even 1-accessible), because it is known that there are 3D configurations with no movable modules on the outside [26].

1.2 Our Results

We develop two very different reconfiguration algorithms, establishing two different universality results in the 2-accessible sliding-cubes model:

1. Allowing extra modules, we show how to construct *any* connected polycube from a straight line, and thus how to reconfigure between any two connected polycubes [Section 2]. The total number of extra modules is linear in the number of modules in the polycube. We also give a negative result that there are structures which are impossible to reconfigure between in the 3-loose sliding-cubes model, thus showing that our algorithm’s result is tight.

2. Without extra modules, we show how to construct any connected polycube having “external feature size” at least 2, and thus how to reconfigure between any two such polycubes [Section 3]. Here we define *external feature size at least k* as follows:
 - a. Every empty $1 \times 1 \times 1$ cube Q is contained in an empty $k \times k \times k$ cube \hat{Q} (see Figure 5 (left)); and
 - b. For every pair of edge-adjacent empty $1 \times 1 \times 1$ cubes Q_1 and Q_2 , there exist empty $k \times k \times k$ cubes \hat{Q}_1 and \hat{Q}_2 containing Q_1 and Q_2 respectively, such that we can continuously slide \hat{Q}_1 into \hat{Q}_2 by axis-parallel unit slides while preserving emptiness of the intermediate $k \times k \times k$ cube and remaining within the bounding box of $\hat{Q}_1 \cup \hat{Q}_2$ (see Figure 5 (middle and right)).

As already mentioned, 2-loose sliding is a slightly stricter constraint than in the pivoting-cubes model. In our second result we build upon the techniques developed for both, the sliding-cube and the pivoting-cube models.

The second construction has a useful additional property called *monotonicity*. Assume we start from a line or box of modules, and the goal is to assemble the desired polycube adjacent to this starting configuration. Then we move the modules in order, and once a module stops moving, we never move it again. Monotonicity implies both accessibility and the lack of extra modules. Furthermore, monotonicity tells us that the assembly process is particularly efficient to simulate with one moving robot and many passive modules: the robot simply needs to double the motion of each module (once to move the module in place, and then in reverse to get the next module).

Our algorithm descriptions focus on the case $k = 2$, as it is the simplest case where the model differs from past work, and as an ARMADAS robot can fit within a $2 \times 2 \times 2$ cube.

2 Universality with Extra Modules: 3D Printing

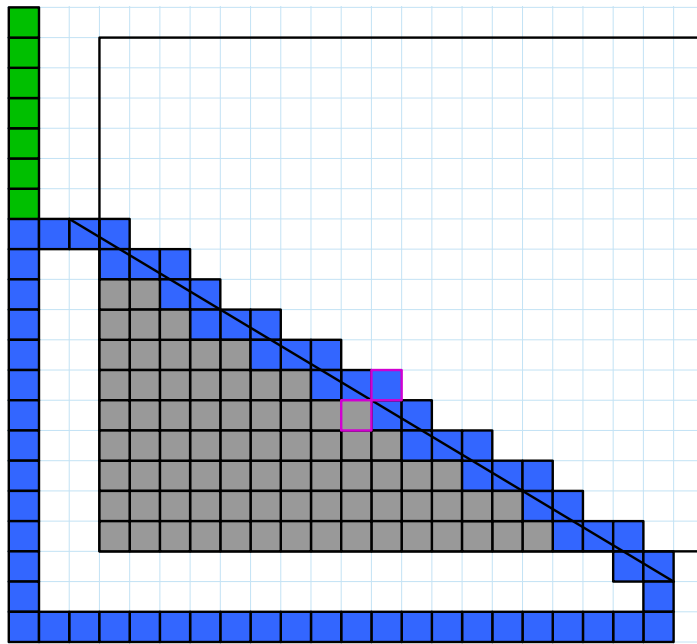
In this section, we will give a 2-accessible algorithm to disassemble any connected structure using extra “scaffolding” modules. More precisely, given an initial configuration T of n modules, and a line of $O(n)$ extra modules attached to it, the algorithm will reconfigure the structure into a single line of modules. The intuition behind the algorithm is to “3D print” the structure in reverse by gradually moving a sweep plane through the structure. The sweep plane is filled with modules to preserve the connectivity of the structure, allowing the modules of T to be removed one at a time. We will first describe a simpler version of the algorithm for two-dimensional structures to give intuition.

2.1 2D

Let $T \subseteq \mathbb{Z}^2$ be the shape we want to disassemble and $U \subseteq \mathbb{Z}^2$ be an axis-aligned rectangle which contains T . We will reconfigure it into a single long line L .

The main idea is to sweep U with a diagonal line of scaffolding, placing modules in front of it if they are not already present, and removing modules behind it. We use a possibly counterintuitive slope of 3 : 5 for the sweep line. As it will become clear later, it is hard to maintain connectivity of the intermediate structure with simpler slopes. In particular, a simpler horizontal, vertical or 1 : 1 diagonal slope does not allow us to “dig” a small hole in the sweep line to remove a module from behind it without either temporarily breaking connectivity or moving a module that is not 2-accessible.

Let $f(x, y) = 3x + (5 - \varepsilon)y$ for some small $\varepsilon \ll 1/n$. Our diagonal line of scaffolding will consist of all modules which are intersected by the line $f(x, y) = t$ for some t which we gradually decrease to sweep the line across. This is equivalent to sweeping a 3 : 5 slope line



■ **Figure 7** The 2D sweep line approach. Blue squares are part of the sweep line, gray squares are the remaining part of T that has not been deconstructed. (Not all gray squares correspond to existing modules, since T is an arbitrary connected subset.) Purple squares are the next modules to be added or removed. The outer black box is the boundary of U . The green squares are the line L where removed modules are appended.

across, and when it hits several modules simultaneously, tiebreaking in favor of processing the higher y valued ones first. We define an intermediate state R_t to be the union of the following four sets (refer to Figure 7):

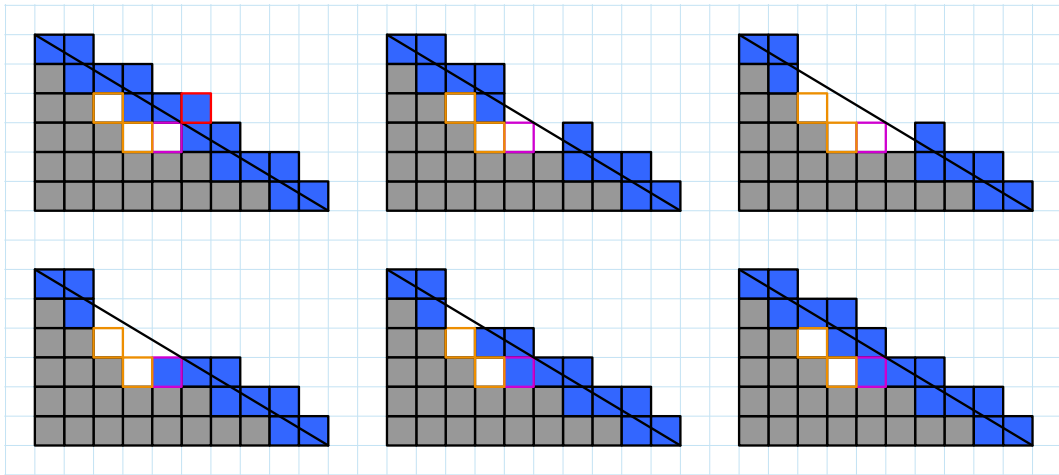
- remainder of the structure $\{(x, y) \in T \mid f(x, y) \leq t\}$,
- a diagonal “sweep line” of modules $\{(x, y) \in U \mid t < f(x, y) \leq t + 8 - \varepsilon\}$,
- a path outside of U connecting the two ends of the sweep line. This is just to ensure the structure remains connected when we remove modules from the sweep line, and
- the portion of L that has been built so far: a line of modules that have been removed from T that is attached to the path outside of U .

► **Observation 1.** *Any 2-accessible module can slide along the exterior of R_t to the end of the line L in $O(n)$ moves.*

Using the above observation, any extra modules that are not part of R_t at time t are placed in the line L . For the rest of this section, whenever we refer to “removing” a module, we mean sliding it to the end of L .

Initially, we construct a bounding box made of the additional modules around U with an extra gap of two units. Furthermore, we connect T to this bounding box. Specifically, we build a path of modules out from the right-most top-most module of T to the upper right corner of the bounding box. This is done simply to ensure the sweep line is connected to T initially (and we can equivalently think of T as containing this additional path).

We are going to gradually decrease t , starting from $R_\infty = T$ and ending at $R_{-\infty} = \emptyset$. As we decrease t , R_t changes only when $t = f(x, y)$ or $t = f(x, y) - 8 + \varepsilon$ for some $(x, y) \in U$, which happens $|U|$ times. More specifically, a module at (x, y) is added to the sweep line



■ **Figure 8** An example of processing a sweep-line event. Reading left to right, this shows the intermediate steps of adding and removing a module from R_t , when both cells outlined in orange are empty. The red outlined module is being removed and the purple outlined one is being added. Other cases are treated similarly; the details can be found in the full version of this paper.

when $t = f(x, y)$, and is removed from it when $t = f(x, y) - 8 + \varepsilon$. Note that, whenever the first condition is met for (x, y) , the second condition is met for $(x + 1, y + 1)$. Thus, each event updating R_t will involve removing one module at $(x + 1, y + 1)$ and adding one module at (x, y) . Consecutive states of R_t differ in only these two modules. We will show that we can always transition from R_t to $R_{t-\varepsilon}$ in a constant number of moves near the sweep line, plus, if necessary, a linear number of moves to take the removed modules out to the end of the line L .

The proof of the following lemma is omitted and can be found in the full version of this paper.

► **Lemma 2.** *There is a sequence of $O(n)$ 2-accessible moves that reconfigures R_t to $R_{t-\varepsilon}$.*

Because each dimension of U is $O(n)$, the sweep line consists of $O(n)$ modules, so we only use $O(n)$ additional modules to deconstruct T .

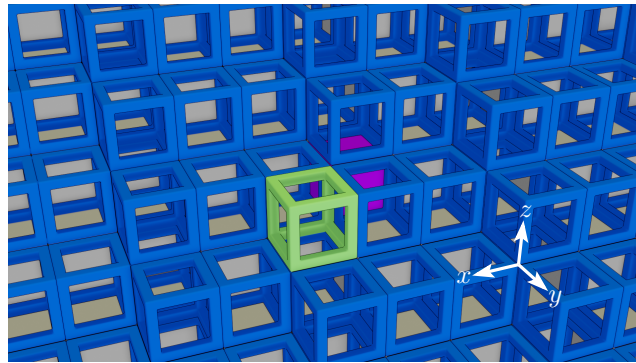
► **Theorem 3.** *Any polyomino shape T can be deconstructed into a line with 2-accessible sliding moves with the help of additional $O(n)$ modules.*

2.2 3D

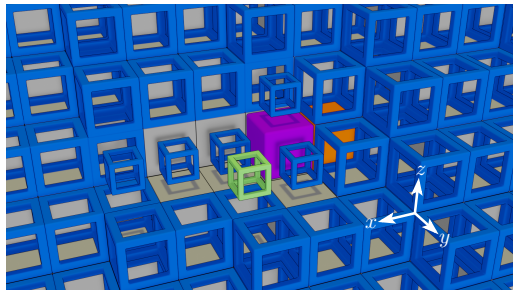
Next we describe the full three-dimensional algorithm for disassembling a structure. Let $T \subseteq \mathbb{Z}^3$ be the shape we want to disassemble, and $U \subseteq \mathbb{Z}^3$ be an axis-aligned bounding box which contains T . Similarly to the 2D case, we sweep a diagonal plane of scaffolding. At each step, we add a module in front of the sweep plane if it is not already present and remove a module from behind the plane.

Define $f(x, y, z) = x + (3 - \varepsilon)y + (3 - \varepsilon^2)z$, for sufficiently small ε . Again, we define R_t to be the set of modules still present in the structure at time t , which is the union of three sets:

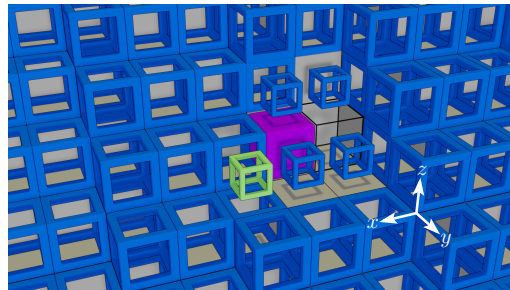
- the remainder of the structure: $\{(x, y, z) \in T \mid f(x, y, z) \leq t\}$,
- the diagonal sweep plane of scaffolding keeping everything connected: $\{(x, y, z) \mid t < f(x, y, z) \leq t + 4 - \varepsilon\}$,



■ **Figure 9** The state of our “3D printing” algorithm before processing an event. The scaffolding plane is shown in blue. Purple cell is at (x, y, z) and a module is to be placed in it; green module is at $(x + 1, y + 1, z)$ and is to be removed.



■ **Figure 10** The solid orange module behind the purple cell is part of T . The small blue and green blocks correspond to the modules that are removed in order to access the purple cell without breaking connectivity.



■ **Figure 11** There is an empty cell behind the purple cell. The small blue and green blocks correspond to the modules that are removed in order to access the purple cell without breaking connectivity.

- the portion of L that has been built so far: a line of modules that have been removed from T that is attached to the path outside of U , and
- additional modules near the boundary of the sweep plane which help preserve connectivity of the sweep plane near the boundary of U : $\{(x, y, z) \mid t < f(x, y, z) \leq t + 6 - 2\varepsilon\}$, when (x, y, z) is outside of U but is within four-unit distance of the boundary of U .

Similarly to the 2D case, as the sweep plane moves, we keep the line L attached to the scaffolding. Whenever a module is removed, it can slide along this connection to the end of L to be deposited.

► **Lemma 4.** *There is a sequence of $O(n)$ 2-accessible moves that reconfigures R_t to $R_{t-\varepsilon}$.*

Proof. As before, we continuously decrease t . Each time R_t changes, up to one module is added to the sweep plane at (x, y, z) and the module at $(x + 1, y + 1, z)$ is removed from it (refer to Figure 9). Removing modules is straightforward: they can slide to the end of L . Adding modules, however, requires some care. When we need to add a module at location (x, y, z) in front of the sweep plane, we “dig” a small hole in the plane, add the new module, and then fill in the hole back.

Next we provide specific steps for processing the event $f(x, y, z) = t$. First, if a module at (x, y, z) already exists in R_t , we simply remove the module at $(x + 1, y + 1, z)$. When a cell (x, y, z) is not occupied and a module needs to be placed in it, we consider the following two cases, based on whether $(x - 1, y, z)$ is present or not.

Case 1: cell $(x - 1, y, z)$ is occupied. See Figure 10.

1. Remove $(x + i, y + 1, z)$ for $i = 1, 0$, and $(x, y, z + 1)$.
2. Remove $(x + i, y, z)$ for $i = 1, 2, 3$.
3. Place $(x + i, y, z)$ for $i = 0, 1, 2, 3$.
4. Place $(x, y + 1, z)$ and $(x, y, z + 1)$.

Case 2: cell $(x - 1, y, z)$ is empty. See Figure 11.

1. Remove $(x + i, y + 1, z)$ for $i = 1, 0, -1$, and $(x + i, y, z + 1)$ for $i = 0, -1$.
2. Place (x, y, z) .
3. Place $(x + i, y + 1, z)$ and $(x + i, y, z + 1)$ for $i = -1, 0$.

Note, that every module that is being removed or added in the steps above is 2-accessible by construction.

When we are outside of U , we will use a different method to add and remove modules from the sweep plane. As the modules of the scaffold that are outside of U are sufficiently removed from T , the empty cells in front of the sweep plane adjacent to them are in fact 2-accessible. Thus, we can simply add a module directly to the front of the sweep plane and remove a module directly from the back side.

Observe that in this case the connectivity of the scaffolding is preserved. Every point (x, y, z) with $f(x, y, z) < t$ that is face-adjacent to a module in the sweep plane maintains the property that at least one of the modules in the sweep plane that it is face-adjacent to is present at all points during the process. This means that if the structure was connected before this step of the algorithm, it remains connected during this step, and will still be connected afterward. ◀

Each dimension of U is $O(n)$. However, because the sweep plane is two-dimensional, this means that our algorithm requires $O(n^2)$ additional modules. We can reduce the number of modules needed by reducing the size of U . Instead of using a full bounding box, we construct U as follows. Consider a discretization of the lattice grid into $2 \times 2 \times 2$ metacells. For each module in T , consider the line passing through the center of the module perpendicular to the sweep plane. We let U be the intersection of the bounding box of T and union of all metacells that are pierced by any such line.

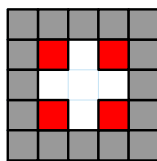
Because we maintain the 4-module offset of the boundary of U be padded with an extra layer of modules in the front of the sweep plane, our sweep plane stays connected at each step of the reconfiguration regardless of the shape of the boundary of U . By construction of U , as it is made of $2 \times 2 \times 2$ metacells, the empty cells, adjacent to the front of the sweep plane, within distance 4 of the boundary of U are necessarily 2-accessible. Since the original algorithm does not depend on the specific shape of U but only the fact that the edge modules are 2-accessible, the correctness of the algorithm follows. The size of the intersection of our sweep plane with U is $O(n)$ by construction, so we now only need $O(n)$ additional modules.

► **Theorem 5.** *Any polycube shape T can be deconstructed into a line with 2-accessible sliding moves with the help of additional $O(n)$ modules.*

2.3 Impossibility of 3-loose algorithm

In this section we describe a structure which cannot be reconfigured into a line with any 3-loose algorithm. We will first describe a 2D version and then generalize to a 3D version.

Consider the structure in Figure 12. It consists of a hollow 5×5 square, as well as the four modules in the corners of a concentric 3×3 square (marked in red). Suppose we can disassemble this structure. Consider the first time we place or remove a module in the central



■ **Figure 12** 2D configuration that cannot be disassembled with a 3-loose algorithm. The red blocks cannot be removed until at least one other red block is removed.

3×3 square. We cannot place a module anywhere inside the 3×3 square, because it would be blocked by red modules. So we must remove a red module. Then this red module must be the only module in some 3×3 square. It is not hard to show that this module cannot have any neighbors, which violates connectivity.

In 3 dimensions, we instead use a hollow $5 \times 5 \times 5$ with 8 modules in the corners of a $3 \times 3 \times 3$ cube. We can use a similar argument to show that no module can be placed or removed inside the central $3 \times 3 \times 3$ cube.

3 Universality without Extra Modules

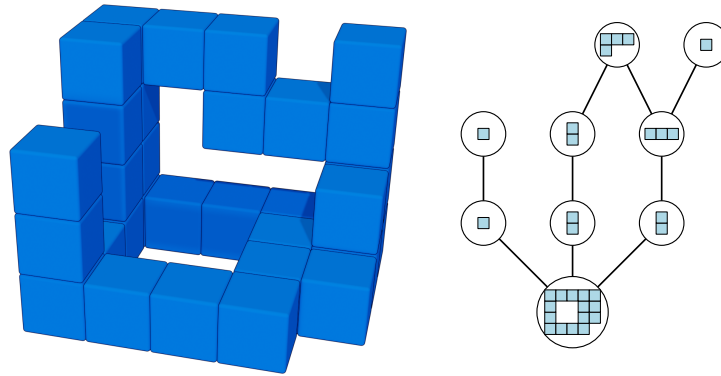
In this section we show how to reconfigure a modular robot, whose shape satisfies the property of external feature size at least 2, into a line. The resulting reconfiguration will consist of 2-accessible and monotone moves (every sliding move will have a sufficient amount of empty space around it, and each module moves only once in a continuous motion from its starting to its target position). Reversing the sequence moves results in a schedule for the construction of the given structure starting from a line of modules.

The approach we take is similar to the one for the pivoting-cube model, presented in [34] and later further developed in [17, 24]. We deconstruct the robot structure slice by slice (parallel to the horizontal plane), ensuring the connectivity of the intermediate structure and the invariant of external feature size at least 2. In our algorithm, the choice of which slice to deconstruct is made in the same way as in [34, 17, 24]. The difference of our algorithm with these approaches, and its main difficulty, lies in deciding in which order to deconstruct (partially or fully) a given slice, such that the requirements on the connectivity and the external feature size are satisfied for the intermediate structures.

Slice graph. We adapt the definition of a slice graph from [34]. Let $V_{z=k}$ denote the subset of nodes of the lattice with the z -coordinate fixed to k . Let V_R denote the subset of nodes of the lattice which contain a module in an intermediate configuration R . Define a *slice graph* $G_s(V_s, E_s)$ of R in the following way. The nodes V_s of G_s correspond to the maximally connected components of the modules with the same z -coordinate, such that these components have at least one module adjacent to the empty outer space. That is, each connected component of the induced graphs on $V_R \cap V_{z=k}$ (for all k), that has a module adjacent to an empty cell of an outer empty space, is added to V_s . Two nodes in V_s are connected with an edge if the corresponding slices contain (vertically) adjacent modules (see Figure 13).

A slice $s \in V_s$ is *locally maximal (minimal)*, if all the adjacent slices of s in G_s contain modules with only lower (higher) z -coordinate than s .

Outline of the algorithm. Consider the initial configuration T with external features of size at least 2. Let s_0 be the slice in G_s with the globally maximum z -coordinate. Select an arbitrary module m_0 from s_0 . Define a configuration L to be formed by a vertical line of n



■ **Figure 13** A robot configuration on the left, and the corresponding slice graph on the right.

modules with m_0 as the bottom-most module, i.e., all the other modules have the same x - and y -coordinates as m_0 , and have z -coordinates larger than z -coordinate of m_0 . We will prove that we can reconfigure from T to L in $O(n^2)$ number of moves.

We iteratively consider a locally extremal outer-surface slice s other than s_0 which is not needed for the connectivity of the current slice graph, and move its modules to the top of the line above m_0 . There are two cases: either removing s disconnects the structure or it does not. If removal of s does not disconnect the robot structure, we simply completely deconstruct s and proceed with the next locally extremal outer-surface slice.

The harder case is when s disconnects the structure. In this case, s must lie on the boundary of a *void*, an enclosed empty space. Furthermore, within this void there must be some modules attached to s which are connected to the rest of the structure only through s . Then, we partially disassemble s while ensuring the connectivity of the intermediate structure, preserving the property of external feature size 2, and connecting the void to the outer empty space.

To summarize, our algorithm consists of the following steps:

1. Construct the slice graph H ;
2. Using H , select a locally extremal outer-surface slice s to deconstruct;
3. Deconstruct s fully (if connectivity is maintained) or partially, update H accordingly;
4. Repeat steps 2 and 3 until L has been constructed.

Step 1: Constructing the slice graph. The definition of a slice graph from [34] does not require that at least one module from each slice is on the outer surface (adjacent to an empty cell of the outer empty space). Their result relies on the assumption that any void, a structure to be deconstructed may have, is convex. Thus, all the slices of the structure have modules that lie on its outer surface. In particular, all the modules of any locally extremal slice lie on the outer surface. In our case, however, the structure may have non-convex voids, and thus some slices (including locally extremal ones) may be “trapped” inside a void. We can only move modules that are on the outer surface of the structure. Thus, to facilitate the choice of a slice to deconstruct, we only maintain the slices in H that are not trapped in a void. That is, we require the nodes of G_s to correspond to the slices with at least one module on the outer surface of the structure.

Step 2: Selecting a slice to deconstruct. We require the slice we select for deconstruction to satisfy two properties: (1) its removal should not disconnect the remaining structure, and (2) it should be locally extremal in the z -direction to give enough space for the modules

to move on its top (or bottom). Note that naively selecting a slice that corresponds to a non-cut node in H may violate property (2), and selecting a top-most or bottom-most slice may violate property (1).

Slice s_0 , containing the node m_0 (the end of the line L) will be the last one to be deconstructed. If there are no other nodes left in H , we deconstruct s_0 . Otherwise, consider the degrees of the nodes in V_s . If there is a node $s \neq s_0$ with degree 1, we select it for deconstruction. Otherwise, select a locally extremal slice s that is furthest away from s_0 in H . Removing s from H does not disconnect the graph. Indeed, otherwise, after the removal of s from H , the component not containing s_0 would have at least two locally extremal slices. At least one of these slices existed in H before removing s , and is further away from s_0 than s . Thus, the lemma follows.

► **Lemma 6.** *If H has more than one slice, there is always a locally extremal slice $s \neq s_0$ in H whose removal does not break the connectivity of H .*

Step 3: Deconstructing a locally extremal slice. Consider a set of empty cells V_e of the empty outer-space component, adjacent to the modules of the structure. Connect two face-adjacent nodes of V_e with an edge, if the corresponding move is 2-loose or is a convex transition consisting of two 2-loose slide steps. Observe, that by definition of the external feature size property, graph G_e is connected. And furthermore, any two nodes of V_e corresponding to face-adjacent cells have an edge connecting them.

► **Observation 7.** *Consider a structure T that has external feature size at least 2, and a top-most node m_0 . Consider an additional module m anywhere on the outer surface of T . Then m can move to the top of m_0 with loose-sliding moves.*

Let s be our locally extremal slice, and let z_s be the value of the z -coordinate of the modules in s . By symmetry, suppose s has no adjacent modules in the positive z direction, thus all the modules adjacent to the modules of s have z -coordinate equal to $z_s - 1$.

Following the notation of [24], we assign colors to the modules of s , depending on whether they have adjacent modules below or not (refer to Figure 14). A module m in s is colored:

- **red** if the cell below m is occupied by some module m' , and the slice containing m' is adjacent to the outer empty component,
- **green** if the cell below m is empty and belongs to the outer component of R ,
- **blue** if the cell below m is empty and does not belong to an outer empty component (i.e., it is a void), and
- **orange** if the cell below m is occupied by some module m' , and the slice containing m' is not adjacent to the outer empty component (i.e., it is enclosed in a void).

We consider two cases, whether the removal of s from the modular structure breaks its connectivity, or not. If the removal of s does not break the connectivity of the structure, we move all the modules of s one by one to the end of L . The proof of the following lemma can be found in the full version of this paper.

► **Lemma 8.** *Suppose that removing a locally extremal slice s of H does not disconnect the modular structure. Then s can be completely deconstructed, and the resulting structure maintains the external-feature-size-2 property.*

Consider now the case when removing s disconnects the modular structure. This is the case if the structure contains a void, and the void has trapped modules inside, attached to s . In this case we no longer can completely deconstruct s , and our goal instead is to cut a hole into at least one void without breaking connectivity and while preserving the external feature size of at least 2.

34:14 Reconfiguration Algorithms for Cubic Modular Robots

To do so, we define a directed graph G_s on the modules of s . All pairs of face-adjacent modules in s are connected with a directed edge. Using G_s , we select which modules from s are to be removed at this step of the algorithm. In particular, all the modules of s that are reachable from orange modules in G_s remain in the slice. All the other modules are deconstructed. Below, we argue that this preserves the external-feature-size-2 property, and eliminates at least one void. Afterwards, we update the slice graph H by adding to it new slices that were trapped inside the eliminated void(s), and proceed to the next iteration of the algorithm.

We construct G_s in the following way. Add all modules of s as nodes in G_s . We call a module of s *reddish* if it has a module in the layer below it (and so is either red or orange in color), and *bluish* if it does not (and thus is either green or blue). Add the following edges to G_s (refer to Figure 14):

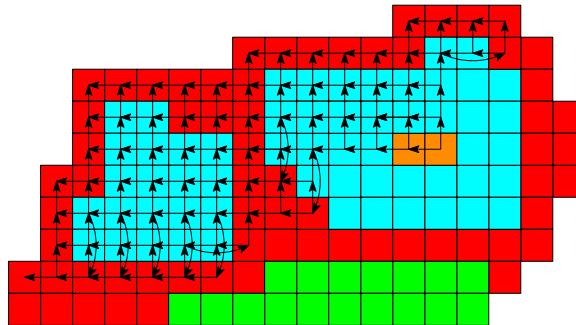
- For two face-adjacent modules with the same y -coordinate, add an edge directed to the left.
- For two face-adjacent modules with the same x -coordinate, add an edge directed upward.
- For a triplet of bluish-bluish-reddish modules oriented left-to-right (or top-to-bottom), add a directed edge from the left-most (top-most) bluish module to the reddish module.

► **Lemma 9.** *If there are modules present at both locations a and b , and a and b are at most 2 units apart in each dimension, then there is a path in the adjacency graph of s from a to b within the bounding box spanned by a and b .*

Proof. Suppose this is the minimal such counterexample. Consider a sequence of empty cells within this bounding box which starts adjacent to a and ends adjacent to b . (If there are no such adjacent empty cells to a and b , then this example was not minimal: we could have instead taken one of the occupied cells adjacent to a or b and gotten a smaller counterexample). Now we know that each of these cells is contained in an empty $2 \times 2 \times 2$ region. Consider this sequence of $2 \times 2 \times 2$ regions. It must be possible to slide between each adjacent pair of modules of empty space because we have external feature size 2. However, this is not going to be possible because we cannot fit an empty $2 \times 2 \times 2$ cube between a and b . ◀

Lemma 9 is the key reason why we use external feature size 2. It follows directly that none of the $1 \times 1 \times 3$, $1 \times 2 \times 2$, and $1 \times 2 \times 3$ forbidden patterns in [34] will be present in our structure, and also ensures that every module that is accessible is 2-accessible.

The proof of the following lemma can be found in the full version of this paper.



■ **Figure 14** Extremal slice with its modules colored according to the adjacency with the nodes in the slice below. Component of the directed graph G_s of modules reachable from orange modules, used in Lemma 9.

► **Lemma 10.** *Every minimal path between any module and a blueish module is bitonic in both x and y : it never goes right after going left and it never goes down after going up.*

► **Corollary 11.** *All blueish cells reachable from an orange cell are either strictly above it or strictly to the left of it.*

Proof. Consider the shortest path to some cell. By construction of G_s , the first move must be to the left or up. If it has non-zero leftward component, then it can never go right. If it has non-zero upward component, then it can never go down. ◀

► **Corollary 12.** *There is an orange module such that a 2×2 square directly below and to the right of it is unreachable.*

► **Corollary 13.** *If two modules a and b on the same row or column are reachable from an orange module, then every module in between also is.*

► **Lemma 14.** *Any two $2 \times 2 \times 2$ edge-adjacent empty regions can be slid together until they overlap in at least one cell.*

Proof. Suppose for contradiction that we have two such edge-adjacent $2 \times 2 \times 2$ empty cubes that cannot be slid closer together. This means there is a $2 \times 2 \times 1$ pattern of diagonally opposite modules with empty space at the other two corners. Suppose we created such a pattern containing one of the modules we removed. Because the region we removed is convex by Corollary 13, it must contain a module from the layer below. In particular, the removed cell from this layer must be red, and there must be an adjacent blueish cell that is not removed. However, in our directed graph there is always an edge from a blue cell to an adjacent red cell, so this is impossible. ◀

► **Lemma 15.** *Every removed blue cell is part of a 2×2 removed square of blue cells.*

Proof. Suppose that a removed blue module is not part of a blue 2×2 disassembled square. Then it must have two neighbors on opposite sides that are each either reddish or unremoved blue. It cannot have two unremoved blue neighbors on each side because of the convexity of the removed area the algorithm generates. It cannot have two reddish neighbors on each side because that would violate the external feature size beforehand. Finally, it cannot have a unremoved blue pixel on one side and a reddish on the other side because the rules that generate the graph would have connected the blue to the reddish neighbor. ◀

► **Lemma 16.** *For any pair of overlapping $2 \times 2 \times 2$ empty cubes, at least one of which was created by removing a module from this layer, we can continuously slide one into the other while preserving emptiness.*

Proof. Because every removed cube is part of a 2×2 removed square of blue pixels by Lemma 15, every new empty space is part of some empty $2 \times 2 \times 2$ cube.

Let the deconstructed layer have $z = z_s$. Consider two overlapping $2 \times 2 \times 2$ empty cubes \hat{Q}_1 and \hat{Q}_2 after partially deconstructing s . If both cubes reside in $z = z_s - 1$ and $z = z_s$, then we consider cubes \hat{Q}'_1 and \hat{Q}'_2 that are the projection of \hat{Q}_1 and \hat{Q}_2 to layers $z = z_s - 1$ and $z = z_s - 2$. Due to the external feature size, \hat{Q}'_1 and \hat{Q}'_2 must both have been empty and it must have been possible to slide between them. We project that motion back up to \hat{Q}_1 and \hat{Q}_2 and get a motion that sweeps between the two cubes.

If both \hat{Q}_1 and \hat{Q}_2 reside in $z = z_s$ and $z = z_s + 1$, we consider cases based on the difference in their x and y coordinates. If they share the same x or y coordinates, then there is a direct motion between them maintaining the shared coordinate. If one of them is larger

in both x and y , we know that their bounding box is empty by the convexity of the removed area, so any motion suffices. If one is smaller in x and larger in y , then we slide it first in the increasing x direction, and then in the decreasing y direction.

If, w.l.o.g., \hat{Q}_1 resides in $z = z_s$ and $z = z_s - 1$, and \hat{Q}_2 in $z = z_s$ and $z = z_s + 1$, then we slide \hat{Q}_1 up one layer first, then proceed with a similar argument to the case above. ◀

By Lemmas 14 and 16, everything must still have external feature size at least 2.

Finally, by Corollary 12, we have made a hole in slice s , which allows us to access modules inside the void. We have made progress by opening up at least one void. Since at each step of the algorithm we either clear one slice or open at least one void, and there are finitely many voids in the structure, we must eventually terminate with the entire shape deconstructed. Because each module needs to move a distance of at most $O(n)$, and each module is only moved once, the total number of moves is at most $O(n^2)$.

► **Theorem 17.** *A modular structure with external-feature size at least 2 can be reconfigured into a line in $O(n^2)$ 2-accessible moves.*

4 Open Problems

The main open question is how many extra modules we need to achieve universal reconfiguration in the k -accessible sliding-cubes model. Our solution in Section 2 uses $\Theta(n)$ extra modules in the worst case. But plausibly $O(1)$ extra modules suffice via a different method; such a result was previously obtained for the pivoting-squares model [3].

Another open problem is whether universal reconfiguration is possible for the k -loose sliding-cubes model – without the k -accessible constraint. In particular, this would require handling complex 3D configurations with no movable modules on the outside [26]. Previous solutions in the sliding-cubes model [27] are not loose.

References

- 1 Zachary Abel, Hugo Akitaya, Matias Korman, Scott Kominers, and Frederick Stock. A universal in-place reconfiguration algorithm for sliding cube-shaped robots in quadratic time. To appear at the 40th International Symposium on Computational Geometry (SoCG), 2024.
- 2 Zachary Abel and Scott D. Kominers. Pushing hypercubes around, 2008. [arXiv:0802.3414v2](https://arxiv.org/abs/0802.3414v2).
- 3 Hugo A. Akitaya, Esther M. Arkin, Mirela Damian, Erik D. Demaine, Vida Dujmović, Robin Flatland, Matias Korman, Belén Palop, Irene Parada, André van Renssen, and Vera Sacristán. Universal reconfiguration of facet-connected modular robots by pivots: The $O(1)$ musketeers. *Algorithmica*, 83(5):1316–1351, 2021. doi:10.1007/s00453-020-00784-6.
- 4 Hugo A. Akitaya, Erik D. Demaine, Andrei Gonczi, Della H. Hendrickson, Adam Hesterberg, Matias Korman, Oliver Kortén, Jayson Lynch, Irene Parada, and Vera Sacristán. Characterizing universal reconfigurability of modular pivoting robots. In *Proc. 37th International Symposium on Computational Geometry (SoCG)*, pages 10:1–10:20, 2021. doi:10.4230/LIPIcs.SoCG.2021.10.
- 5 Hugo A. Akitaya, Erik D. Demaine, Matias Korman, Irina Kostitsyna, Irene Parada, Willem Sonke, Bettina Speckmann, Ryuhei Uehara, and Jules Wulms. Compacting squares: Input-sensitive in-place reconfiguration of sliding squares. In *Proc. 18th Scandinavian Symposium and Workshops on Algorithm Theory (SWAT)*, volume 227 of *Leibniz International Proceedings in Informatics (LIPIcs)*, pages 4:1–4:19, 2022. doi:10.4230/LIPIcs.SWAT.2022.4.
- 6 Greg Aloupis, Nadia Benbernou, Mirela Damian, Erik D. Demaine, Robin Flatland, John Iacono, and Stefanie Wührer. Efficient reconfiguration of lattice-based modular robots. *Computational Geometry: Theory and Applications*, 46(8):917–928, October 2013. doi:10.1016/j.comgeo.2013.03.004.

- 7 Greg Aloupis, Sébastien Collette, Mirela Damian, Erik D. Demaine, Dania El-Khechen, Robin Flatland, Stefan Langerman, Joseph O'Rourke, Val Pinciu, Suneeta Ramaswami, Vera Sacristán, and Stefanie Wuhler. Realistic reconfiguration of crystalline (and telecube) robots. In *Proceedings of the 8th International Workshop on the Algorithmic Foundations of Robotics (WAFR 2008)*, volume 57 of *Springer Tracts in Advanced Robotics*, pages 433–447, Guanajuato, México, December 7–9 2008.
- 8 Greg Aloupis, Sébastien Collette, Mirela Damian, Erik D. Demaine, Robin Flatland, Stefan Langerman, Joseph O'Rourke, Suneeta Ramaswami, Vera Sacristán, and Stefanie Wuhler. Linear reconfiguration of cube-style modular robots. *Computational Geometry: Theory and Applications*, 42(6–7):652–663, August 2009.
- 9 Greg Aloupis, Sébastien Collette, Erik D. Demaine, Stefan Langerman, Vera Sacristán, and Stefanie Wuhler. Reconfiguration of cube-style modular robots using $O(\log n)$ parallel moves. In *Proceedings of the 19th Annual International Symposium on Algorithms and Computation (ISAAC 2008)*, pages 342–353, Gold Coast, Australia, December 15–17 2008.
- 10 Greg Aloupis, Sébastien Collette, Mirela Damian, Erik D. Demaine, Robin Flatland, Stefan Langerman, Joseph O'Rourke, Val Pinciu, Suneeta Ramaswami, Vera Sacristán, and Stefanie Wuhler. Efficient constant-velocity reconfiguration of crystalline robots. *Robotica*, 29(1):59–71, 2011. doi:10.1017/S026357471000072X.
- 11 Byoung Kwon An. EM-Cube: Cube-shaped, self-reconfigurable robots sliding on structure surfaces. In *Proc. IEEE International Conference on Robotics and Automation (ICRA)*, pages 3149–3155, 2008. doi:10.1109/ROBOT.2008.4543690.
- 12 Nora Ayanian, Paul J. White, Ádám Hálász, Mark Yim, and Vijay Kumar. Stochastic control for self-assembly of XBots. In *Proc. ASME International Design Engineering Technical Conferences and Computers and Information in Engineering Conference (IDETC-CIE)*, pages 1169–1176, 2008. doi:10.1115/DETC2008-49535.
- 13 Nadia M. Benbernou. Geometric algorithms for reconfigurable structures. PhD thesis, Massachusetts Institute of Technology, 2011.
- 14 Kenneth C. Cheung and Neil Gershenfeld. Reversibly assembled cellular composite materials. *Science*, 341(6151):1219–1221, 2013.
- 15 Chih-Jung Chiang and Gregory S. Chirikjian. Modular robot motion planning using similarity metrics. *Autonomous Robots*, 10:91–106, 2001. doi:10.1023/A:1026552720914.
- 16 Adrian Dumitrescu and János Pach. Pushing squares around. *Graphs and Combinatorics*, 22:37–50, 2006. doi:10.1007/s00373-005-0640-1.
- 17 Daniel Feshbach and Cynthia Sung. Reconfiguring non-convex holes in pivoting modular cube robots. *IEEE Robotics and Automation Letters*, 6(4):6701–6708, 2021. doi:10.1109/LRA.2021.3095030.
- 18 Robert Fitch, Zack Butler, and Daniela Rus. Reconfiguration planning for heterogeneous self-reconfiguring robots. In *Proc. IEEE/RSJ International Conference on Intelligent Robots and System (IROS)*, pages 2460–2467, 2003. doi:10.1109/IROS.2003.1249239.
- 19 Christine E. Gregg, Damiana Catanoso, Olivia Irene B. Formoso, Irina Kostitsyna, Megan E. Ochalek, Taiwo J. Olatunde, In Won Park, Frank M. Sebastianelli, Elizabeth M. Taylor, Greenfield T. Trinh, and Kenneth C. Cheung. Ultralight, strong, and self-reprogrammable mechanical metamaterials. *Science Robotics*, 9(86):eadi2746, 2024. doi:10.1126/scirobotics.adi2746.
- 20 Christine E. Gregg, Joseph H. Kim, and Kenneth C. Cheung. Ultra-light and scalable composite lattice materials. *Advanced Engineering Materials*, 20(9):1800213, 2018.
- 21 Kazuo Hosokawa, Takehito Tsujimori, Teruo Fujii, Hayato Kaetsu, Hajime Asama, Yoji Kuroda, and Isao Endo. Self-organizing collective robots with morphogenesis in a vertical plane. In *Proc. IEEE International Conference on Robotics and Automation (ICRA)*, pages 2858–2863, 1998. doi:10.1109/ROBOT.1998.680616.

- 22 Benjamin Jenett, Amira Abdel-Rahman, Kenneth Cheung, and Neil Gershenfeld. Material-Robot System for Assembly of Discrete Cellular Structures. *IEEE Robotics and Automation Letters*, 4(4):4019–4026, October 2019. doi:10.1109/LRA.2019.2930486.
- 23 Irina Kostitsyna, Tim Ophelders, Irene Parada, Tom Peters, Willem Sonke, and Bettina Speckmann. Optimal in-place compaction of sliding cubes. Submission to SWAT, 2024.
- 24 Lloyd E. Lo-Wong. Reconfiguration of pivoting modular robots. MSc thesis, Technical University Eindhoven, 2021.
- 25 Othon Michail, George Skretas, and Paul G. Spirakis. On the transformation capability of feasible mechanisms for programmable matter. *Journal of Computer and System Sciences*, 102:18–39, 2019. doi:10.1016/j.jcss.2018.12.001.
- 26 Tillmann Miltzow, Irene Parada, Willem Sonke, Bettina Speckmann, and Jules Wulms. Hiding sliding cubes: Why reconfiguring modular robots is not easy. In *Proc. 36th International Symposium on Computational Geometry (SoCG)*, volume LIPIcs 164, pages 78:1–78:5, 2020. doi:10.4230/LIPIcs.SoCG.2020.78.
- 27 Joel Moreno. In-place reconfiguration of lattice-based modular robots. Bachelor’s thesis, Universitat Politècnica de Catalunya, 2019.
- 28 Joel Moreno and Vera Sacristán. Reconfiguring sliding squares in-place by flooding. In *Proc. 36th European Workshop on Computational Geometry (EuroCG)*, pages 32:1–32:7, 2020.
- 29 Irene Parada, Vera Sacristán, and Rodrigo I. Silveira. A new meta-module design for efficient reconfiguration of modular robots. *Autonomous Robots*, 45(4):457–472, 2021. doi:10.1007/s10514-021-09977-6.
- 30 In-Won Park, Damiana Catanoso, Olivia Formoso, Christine Gregg, Megan Ochalek, Taiwo Olatunde, Frank Sebastianelli, Pascal Spino, Elizabeth Taylor, Greenfield Trinh, and Kenneth Cheung. Soll-e: A module transport and placement robot for autonomous assembly of discrete lattice structures. In *2023 IEEE/RSJ International Conference on Intelligent Robots and Systems (IROS)*. IEEE, 2023.
- 31 John Romanishin, Kyle Gilpin, and Daniela Rus. M-blocks: Momentum-driven, magnetic modular robots. In *Proceedings of the 2013 IEEE/RSJ International Conference on Intelligent Robots and Systems (IROS 2013)*, pages 4288–4295, Tokyo, Japan, November 2013. IEEE. doi:10.1109/IROS.2013.6696971.
- 32 Daniela Rus and Masette Vona. A physical implementation of the self-reconfiguring crystalline robot. In *Proc. IEEE International Conference on Robotics and Automation (ICRA)*, pages 1726–1733, 2000. doi:10.1109/ROBOT.2000.844845.
- 33 John W. Suh, Samuel B. Homans, and Mark Yim. Telecubes: mechanical design of a module for self-reconfigurable robotics. In *Proc. 2002 IEEE International Conference on Robotics and Automation (ICRA)*, pages 4095–4101, 2002. doi:10.1109/ROBOT.2002.1014385.
- 34 Cynthia Sung, James Bern, John Romanishin, and Daniela Rus. Reconfiguration planning for pivoting cube modular robots. In *Proc. 2015 IEEE International Conference on Robotics and Automation (ICRA)*, pages 1933–1940, 2015. doi:10.1109/ICRA.2015.7139451.
- 35 Yuzuru Terada and Satoshi Murata. Automatic Assembly System for Modular Structure. In *Proceedings of the 22nd International Symposium on Automation and Robotics in Construction*, Ferrara, Italy, September 2005. doi:10.22260/ISARC2005/0028.
- 36 Mark Yim, Wei-Min Shen, Behnam Salemi, Daniela Rus, Mark Moll, Hod Lipson, Eric Klavins, and Gregory S. Chirikjian. Modular self-reconfigurable robot systems. *IEEE Robotics & Automation Magazine*, 14(1):43–52, 2007. doi:10.1109/MRA.2007.339623.